

Bose-Einstein Correlations in Multihadron Events at LEP

C. Ciocca, M. Cuffiani, G. Giacomelli

Dip. di Fisica of the University of Bologna and INFN Sezione di Bologna, I-40127 Bologna, Italy;

ciocca@bo.infn.it, cuffiani@bo.infn.it, giacomelli@bo.infn.it

Invited paper at the “Ninth Workshop on Non Perturbative QCD”

Institut d’Astrophysique de Paris, Paris, France, 4-8 June 2007

Abstract. Bose-Einstein correlations in pairs of identical particles were analyzed in e^+e^- multihadron annihilations at ~ 91.2 GeV at LEP. The first studies involved identical charged pions and the emitting source size was determined. Then the study of charged kaons suggested that the radius depends on the mass of the emitted particles. Subsequently the dependence of the source radius on the event multiplicity was analyzed. The study of the correlations in neutral pions and neutral kaons extended these concepts to neutral particles. The shape of the source was analyzed in 3 dimensions and was found not to be spherically symmetric. In recent studies at LEP the correlations were analyzed in intervals of the average pair transverse momentum and of the pair rapidity to study the correlations between the pion production points and their momenta (position-momentum correlations). The latest e^+e^- data are consistent with an expanding source.

1 Introduction

Bose-Einstein Correlations (BECs) are a quantum mechanical phenomenon which manifests in final multihadron states as an enhanced probability for identical bosons to be emitted with small relative four momentum Q , compared with non identical bosons under similar kinematic conditions [1, 2, 3]. From the measured effect it is possible to determine the space time dimensions of the boson-emitting source. The BEC effect arises from the ambiguity of path between sources and detectors and the requirement to symmetrise the wave function of two or more identical bosons.

In 1954 the radioastronomers R. Hanbury-Brown and R. Q. Twiss proposed a new interferometry technique to measure the angular dimension of a star. It required to measure the mixed intensities in two radiotelescopes; the dependence of the correlation on the distance between them yielded the angular diameter of the astronomical source [1]. G. Goldhaber et al applied the same principle in particle physics, in $\bar{p}p$ annihilations into two identical charged pions, obtaining the radius of the emitting source, ~ 1 fm [2].

The first LEP analyses on BECs concerned identical charged pions, assuming a spherical emission source and yielded the size of the source ($R \sim 1$ fm) and the chaoticity parameter [3, 4]. Neutral π^0 were then considered [5]. Then the study was extended to neutral and charged kaons in order to determine if the source radius depends on the mass of the emitted particles [6, 7].

Further analyses were performed to establish if the emitting source radius depends on the particle multiplicity [8]. Other studies involved the search for BE correlations in multipions [9].

BECs were studied in two and three dimensions and one discovered that the emitting source is not spherical [10]. Many studies were made for WW correlations [11] and also in ν interactions [12]. Finally they involved the study of expanding sources and trials to determine the emission time [13].

We shall make a brief survey of these studies, concentrating finally on the very recent works which prove that even in e^+e^- collisions one has expanding sources.

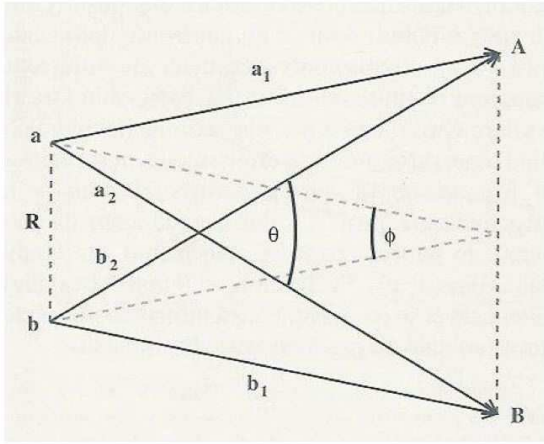


Figure 1: Scheme of a measurement of BECs. a, b are two sources separated by a distance R ; A, B are two detectors separated by a distance L . The emitted particles go from sources to detectors as $a \rightarrow A, b \rightarrow B$ or as $a \rightarrow B, b \rightarrow A$. In astronomy $L \ll R$, in particle physics $L \gg R$.

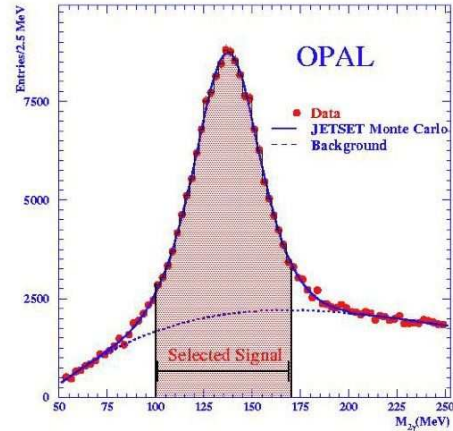


Figure 2: Distribution of two-photon invariant mass, $M_{2\gamma}$. The smooth curves are the total Monte Carlo expectation (solid line) and the background expectation (dashed line). The shaded region is the selected window for the π^0 signal.

2 Experimental Procedure

A detailed description of the OPAL experiment may be found in ref [14]. The most important subdetector for BEC studies is the Central Tracking Detector, the Jet Chamber. For π^0 studies we needed also the barrel electromagnetic calorimeter. A sample of 4.3 million multihadronic events from Z^0 decays were used. A set of quality cuts was applied and one used cuts specific for BEC studies.

First, the event thrust axis was computed, using tracks with a minimum of 20 hits in the jet chamber, a minimum transverse momentum of 150 MeV and a maximum momentum of 65 GeV. Clusters in the electromagnetic calorimeter were used for energies exceeding 100 MeV in the barrel or 200 MeV in the endcaps. Only events well contained in the detector were accepted, requiring $|\cos\theta_{\text{thrust}}| < 0.9$, where θ_{thrust} is the polar angle of the thrust axis with respect to the beam axis. Tracks were required to have a maximum momentum of 40 GeV and to originate from the interaction vertex. Electron-positron pairs from photon conversions were rejected. The selected events contained a minimum of five tracks and were reasonably balanced in charge, i.e. $|n_{\text{ch}}^+ - n_{\text{ch}}^-| / (n_{\text{ch}}^+ + n_{\text{ch}}^-) \leq 0.4$, where n_{ch}^+ and n_{ch}^- are the number of positive and negative charge tracks, respectively. About 3.7 million events were left after all cuts. All charged particle tracks that passed the selections were used, the pion purity being approximately 90%.

Since in multihadron events more than 90% of the measured tracks are charged pions, the study of BEC for like-sign charged pion pairs was usually performed without proper particle identification and without purity correction. This choice introduces a small error in the chaoticity parameter λ and in the radius R of the emitting region. However some analyses were performed with properly identified pions. That required some effective cuts on the fraction of the global solid angle acceptance.

For $\pi^0\pi^0$, $K^\pm K^\pm$ and $K^0 K^0$ correlations, particle identification was necessary [5, 6]. Fig. 2 shows the distribution of the two-photon invariant mass and the π^0 event selection.

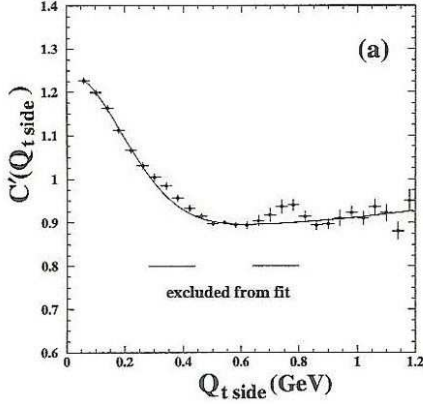


Figure 3: The BEC distribution $C'(Q)$ for charged pions vs $Q_{t\text{side}}$. The smooth solid curve is the fitted correlation function (the excluded regions contain effects from known hadron resonances).

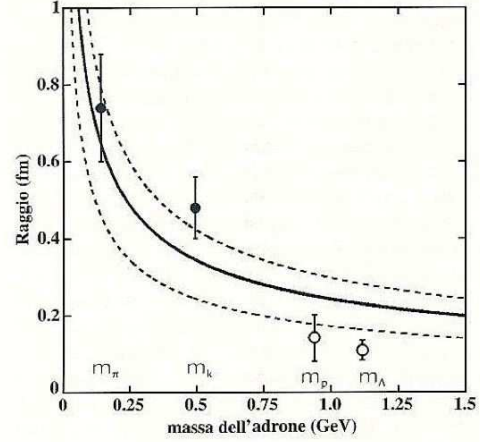


Figure 4: Radius of the emitting region for BECs of 2 identical bosons and for FDCs of 2 identical baryons produced in e^+e^- collisions at LEP.

3 BECs from a static source

BECs in one dimension. The measured BEC function is defined as the ratio $C(Q) = \rho(Q)/\rho_0(Q)$, where Q is a Lorenz-invariant variable expressed in terms of the two pion four momenta p_1 and p_2 as $Q^2 = -(p_1 - p_2)^2$, $\rho(Q) = (1/N)dN/dQ$ is the measured Q distribution of the two pions and $\rho_0(Q)$ is a reference distribution which should contain all the correlations included in $\rho(Q)$, except BECs. For the determination of $\rho_0(Q)$, different methods were used: for identical $\pi^+\pi^+$ and $\pi^-\pi^-$ one used the $\pi^+\pi^-$ sample, but also the event mixing reference sample, where pion pairs are formed from pions belonging to different events; also a Monte Carlo (MC) reference sample without BECs was used.

The correlation distribution $C(Q)$ was parametrised using the Fourier transform of the expression for a static sphere of emitters with a Gaussian density:

$$C(Q) = N(1 + \lambda \exp(-R^2 Q^2))(1 + \delta Q + \epsilon Q^2). \quad (1)$$

λ is the chaoticity parameter, R is the radius of the source, and N a normalization factor. The empirical term $(1 + \delta Q + \epsilon Q^2)$ accounts for the behaviour of the correlation function at high Q due to any remaining long-range correlation. The largest difference among results from different experiments lies in the choice of the reference sample: the statistical errors on R is small, but the systematic uncertainty is large.

Fig 3 shows a typical distribution of $C(Q)$ versus Q ; it is relative to a three dimensional analysis, but the observed features are typical of all BECs: notice the BEC peak at low Q and the tail at large Q ; the solid line is a fit to eq. 1, excluding the Q -intervals indicated in the figure, which contain effects from known hadron resonances.

The same analysis was repeated for KK BECs. A similar analysis was performed on Fermi Dirac Correlations (FDCs) for identical fermions: in this case there is no peak at small values of Q , but a dip. The analysis gives the radius of the emitting regions as shown in Fig. 4. Note that there probably is a decrease of R with increasing mass of the emitted identical particles.

Fig. 5a shows the variation of the emitting radius with the charged multiplicity of the event [8]: there is an increase of about 10% of the radius when the multiplicity increases from 10 to 40 charged hadrons

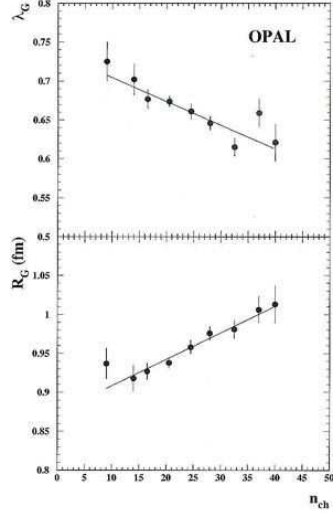


Figure 5: a) Increase of the emitting radius with increasing event multiplicity and b) decrease of λ .

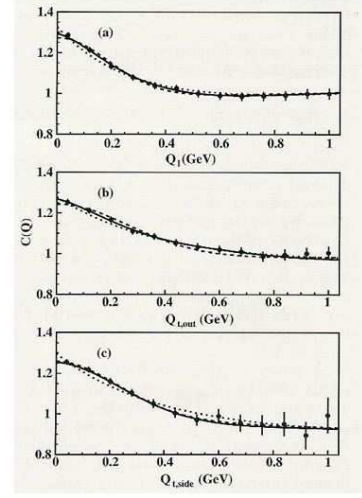


Figure 6: The distributions in $Q_{t_{out}}$ and $Q_{t_{side}}$ are broader than in Q_ℓ : thus $R_\ell > R_{t_{side}} \sim R_{t_{out}}$.

in the final state. This may be related to the number of hadron jets: one has $R_{4jets} > R_{3jets} > R_{2jets}$. Notice that there is a corresponding decrease of the chaoticity parameter, Fig. 5b.

In ref. [10] it was found that there are 3π BECs, that is after removing the effect of 2π correlations on the 3π sample. The present situation is consistent with the relation

$$R_{3\pi} = R_{2\pi}/\sqrt{2} \quad (2)$$

In ref. [9] it was found that there are true multiparticle correlations up to 5π .

BECs in two and three dimensions. Multidimensional static analyses were performed in 3 dimensions using the Longitudinal Center of Mass System (LCMS): the sum of the impulses of the emitted $q\bar{q}$ pair lies in the plane perpendicular to the event axis, defined by the $q\bar{q}$ direction. The components of the 3-dimensional distribution in the longitudinal, out and side projections indicate that the last ones are larger, see Fig. 6. Thus the longitudinal radius is about 20% larger than the transverse radius: the emitting source is ellissoidal, elongated in the $q\bar{q}$ direction.

Comparison of BECs in e^+e^- and Nucleus-Nucleus collisions. Fig. 7 shows the BEC functions in $e^+e^- \rightarrow$ hadrons and Pb Pb \rightarrow hadrons: note how much narrower is the distribution in Pb Pb collisions: the distribution yields a radius $R \simeq 6 - 7$ fm for the emissions of pion pairs.

4 Expanding sources

BECs have been analyzed in Nucleus-Nucleus collisions in order to find evidence for expanding sources due to the formation of a quark-gluon deconfined plasma [15, 16]. Expanding sources may arise in e^+e^- collisions because of string fragmentation [17]. In order to study BECs in non static, expanding sources we analyze the correlation functions

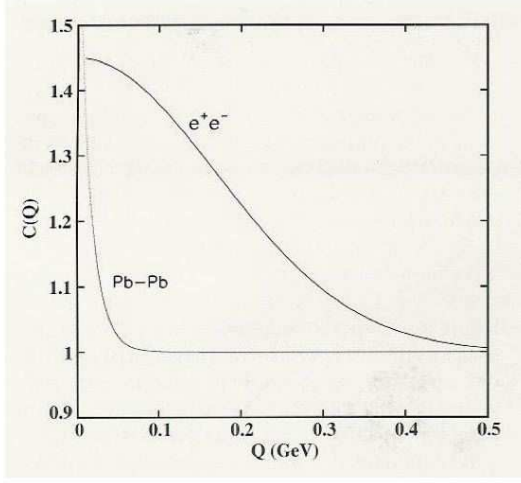


Figure 7: Comparison of the BE Correlation functions for PbPb and e^+e^- collisions.

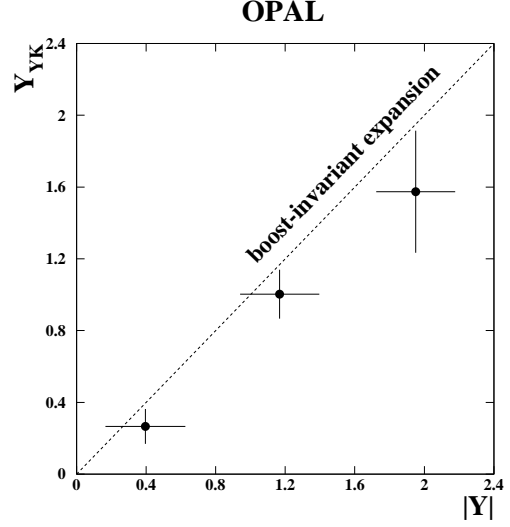


Figure 8: Y_{YK} vs pion pair rapidity Y . Vertical bars include statistical and systematic errors. $Y_{YK}=Y$ corresponds to a source expanding boost-invariantly.

$$C' = \frac{C^{\text{DATA}}}{C^{\text{MC}}} = \frac{N_{\text{like}}^{\text{DATA}}/N_{\text{unlike}}^{\text{DATA}}}{N_{\text{like}}^{\text{MC}}/N_{\text{unlike}}^{\text{MC}}}, \quad (3)$$

in bins of the average pair four-momentum with respect to the event thrust direction

$$k_t = (\vec{p}_{t,1} + \vec{p}_{t,2}) \quad (4)$$

and of the pair rapidity:

$$|Y| = \frac{1}{2} \ln \left[\frac{(E_1 + E_2) + (p_{\ell,1} + p_{\ell,2})}{(E_1 + E_2) - (p_{\ell,1} + p_{\ell,2})} \right] \quad (5)$$

The experimental distributions in $dN/d|Y|$ and dN/dk_t are in good agreement with the distributions from the Jetset Monte Carlo. The dependences of C and C' on K were studied in three bins of $|Y|$ ($0.0 \leq |Y| < 0.8$, $0.8 \leq |Y| < 1.6$, $1.6 \leq |Y| < 2.4$) and five bins of k_t ($0.1 \leq k_t < 0.2$ GeV, $0.2 \leq k_t < 0.3$, $0.3 \leq k_t < 0.4$, $0.4 \leq k_t < 0.5$ and $0.5 \leq k_t < 0.6$ GeV).

Two-dimensional projections of the correlation function $C'(Q_\ell, Q_{t_{\text{side}}}, Q_{t_{\text{out}}})$ for a single bin of $|Y|$ and k_t are shown in Fig. 9a, b. BEC peaks are visible at low $Q_\ell, Q_{t_{\text{side}}}, Q_{t_{\text{out}}}$.

To extract the spatial and temporal extensions of the pion source from the experimental correlation functions, the Bertsch-Pratt (BP)

$$C'(Q_\ell, Q_{t_{\text{side}}}, Q_{t_{\text{out}}}) = N(1 + \lambda e^{-(Q_\ell^2 R_{\text{long}}^2 + Q_{t_{\text{side}}}^2 R_{t_{\text{side}}}^2 + Q_{t_{\text{out}}}^2 R_{t_{\text{out}}}^2 + 2Q_\ell Q_{t_{\text{out}}} R_{\text{long}, t_{\text{out}}}^2)}) F(Q_\ell, Q_{t_{\text{side}}}, Q_{t_{\text{out}}}) \quad (6)$$

and the Yano-Koonin (YK)

$$C'(q_t, q_\ell, q_0) = N(1 + \lambda e^{-(q_t^2 R_t^2 + \gamma^2 (q_\ell - v q_0)^2 R_\ell^2 + \gamma^2 (q_0 - v q_\ell)^2 R_0^2)}) F(q_t, q_\ell, q_0) \quad (7)$$

OPAL

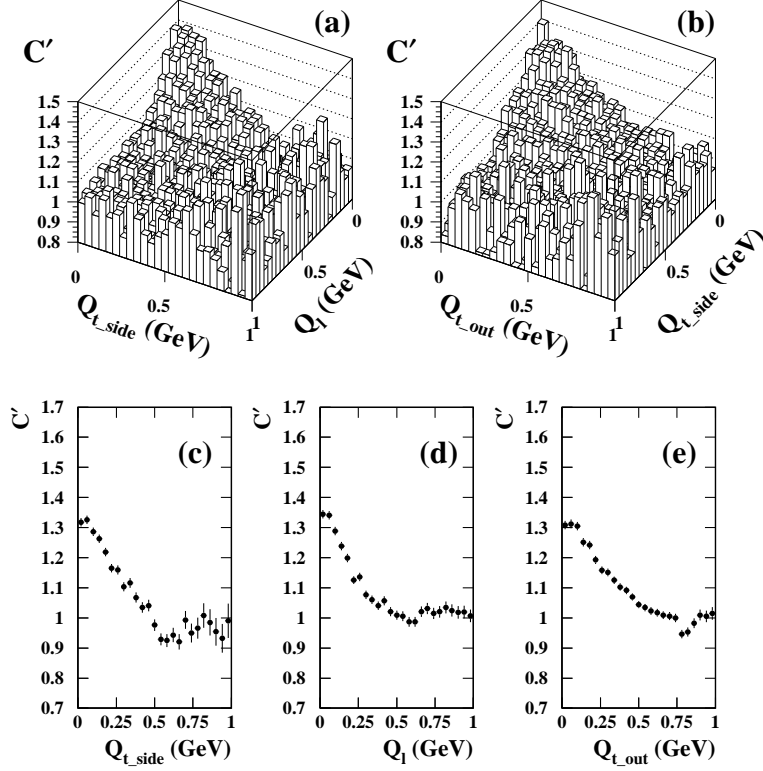


Figure 9: Two-dimensional (a), (b) and one-dimensional (c), (d) and (e) projections of the correlation function $C'(Q_\ell, Q_{t_side}, Q_{t_out})$ for $0.8 \leq |Y| < 1.6$ and $0.3 \leq k_t < 0.4$ GeV. $Q_{t_out} < 0.2$ GeV in (a), $Q_\ell < 0.2$ GeV in (b). In (c), (d), (e) the projections at low values (< 0.2 GeV) of the other variables.

parameterizations were fitted to the measured correlation functions in intervals of k_t and $|Y|$. In both parameterizations, N is a normalization factor, λ is the degree of incoherence of the pion sources, related to the fraction of pairs that interfere. The parameters N and λ , whose product determines the size of the BEC peak, are significantly (anti)correlated. The two functions $F(Q_\ell, Q_{t_side}, Q_{t_out}) = (1 + \epsilon_{long} Q_\ell + \epsilon_{t_side} Q_{t_side} + \epsilon_{t_out} Q_{t_out})$ and $F(q_t, q_\ell, q_0) = (1 + \delta_t q_t + \delta_\ell q_\ell + \delta_0 q_0)$, where ϵ_i and δ_i are free parameters, were introduced in Eq. (6) and (7) to take into account residual long-range two-particle correlations due to energy and charge conservation. The interpretation of the other parameters in Eq. (6), is:

- R_{t_side} and R_{long} are the transverse and longitudinal radii in the longitudinal rest frame of the pair;
- R_{t_out} and the cross-term R_{long, t_out} are a combination of both spatial and temporal extensions of the source. The difference $(R_{t_out}^2 - R_{t_side}^2)$ is proportional to the duration of the particle emission process, and R_{long, t_out} to the source velocity with respect to the pair rest frame.

In the YK frame Eq. (7), where $\gamma = 1/\sqrt{1 - v^2}$, the free parameters are interpreted as follows:

- v is the longitudinal velocity, in units of c , of the source element in the CMS frame;
- R_0 measures the time interval, times c , during which particles are emitted, in the rest frame of the emitter (source element). The limited phase-space available limits the analysis for R_0^2 ;
- R_t and R_ℓ are the transverse and longitudinal radii, in the rest frame of the emitter.

The parameters R_0 , R_t and R_ℓ are evaluated in the rest frame of the source element. The two parameterizations are not independent, so that a comparison between the BP and YK fits is an important test. In the YK picture the source velocity v of each element does not depend on k_t , while it is correlated with the pair rapidity Y . Y_{YK} measures the rapidity of the source element with respect to the c.m. frame $Y_{YK} = \frac{1}{2} \ln [(1+v)/(1-v)]$. A non expanding source corresponds to $Y_{YK} \simeq 0$ for any Y . For a longitudinally boost invariant source (for which the velocity of each element is $v = z/t$, where t is the time elapsed since the collision and z is the longitudinal coordinate of the element) the correlation $Y_{YK} = Y$ is expected as in Fig. 8.

The following relations hold between the BP and YK parameters:

$$R_{t_{\text{side}}}^2 = R_t^2 \quad (8)$$

$$R_{\text{long}}^2 = \gamma_{\text{LCMS}}^2 (R_\ell^2 + \beta_{\text{LCMS}}^2 R_0^2) \quad (9)$$

$$(R_{t_{\text{out}}}^2 - R_{t_{\text{side}}}^2) = \beta_t^2 \gamma_{\text{LCMS}}^2 (R_0^2 + \beta_{\text{LCMS}}^2 R_\ell^2). \quad (10)$$

β_{LCMS} is the velocity of the source element in the LCMS, i.e. with respect to the pair longitudinal rest frame; $\gamma_{\text{LCMS}} = 1/\sqrt{1 - \beta_{\text{LCMS}}^2}$. For a boost-invariant source, $\beta_{\text{LCMS}} = 0$: (9) and (10) become:

$$R_{\text{long}}^2 \simeq R_\ell^2 \quad (11)$$

$$(R_{t_{\text{out}}}^2 - R_{t_{\text{side}}}^2) \simeq \beta_t^2 R_0^2. \quad (12)$$

In Fig. 10 the best-fit BP and YK parameters are compared:

- The longitudinal parameter R_{long}^2 is larger than R_ℓ^2 in all rapidity intervals, Fig. 9(a),(d) and (g). $R_{\text{long}}^2 > R_\ell^2$ corresponds to $\beta_{\text{LCMS}} > 0$, i. e. to a pion source whose expansion is not exactly boost-invariant.
- The equality of the transverse parameters, $R_{t_{\text{side}}}^2 = R_t^2$, is confirmed; there may be deviations at low k_t .
- R_0^2 and $(R_{t_{\text{out}}}^2 - R_{t_{\text{side}}}^2)$ are essentially equal to zero, suggesting that the present technique does not allow to measure the duration of the emission process.

5 Conclusions

We have first summarized the results obtained on BECs in e^+e^- collisions at the Z^0 peak assuming a static source. Then we presented an analysis in bins of the average 4-momentum of the pair. Based on this, the dynamic features of the pion emitting source were investigated in the YK and BP formalisms.

The transverse and longitudinal radii of the pion sources decrease for increasing k_t , indicating the presence of correlations between the particle production points and their momenta. The YK rapidity scales with the pair rapidity, in agreement with a nearly boost-invariant expansion of the pion source. Phase space limitation did not allow the measurement of the duration of the particle emission process.

Similar results have been observed in more complex systems, such as the pion sources created in pp and heavy-ion collisions, which are now complemented with measurements in the simpler hadronic system formed in e^+e^- annihilations. The unexplained similarities between BECs in different reactions might indicate a present limitation of our understanding of these correlations [18].

Acknowledgements. We thank all the members of the OPAL Collaboration, in particular the Bologna members. We acknowledge the contribution of Ms. Anastasia Casoni.

References

- [1] Hanbury-Brown et al., Phil. Mag. 54 (1954) 633; Nature 178 (1956) 1046.
- [2] G. Goldhaber et al., Phys. Rev. 120 (1960) 130.

OPAL

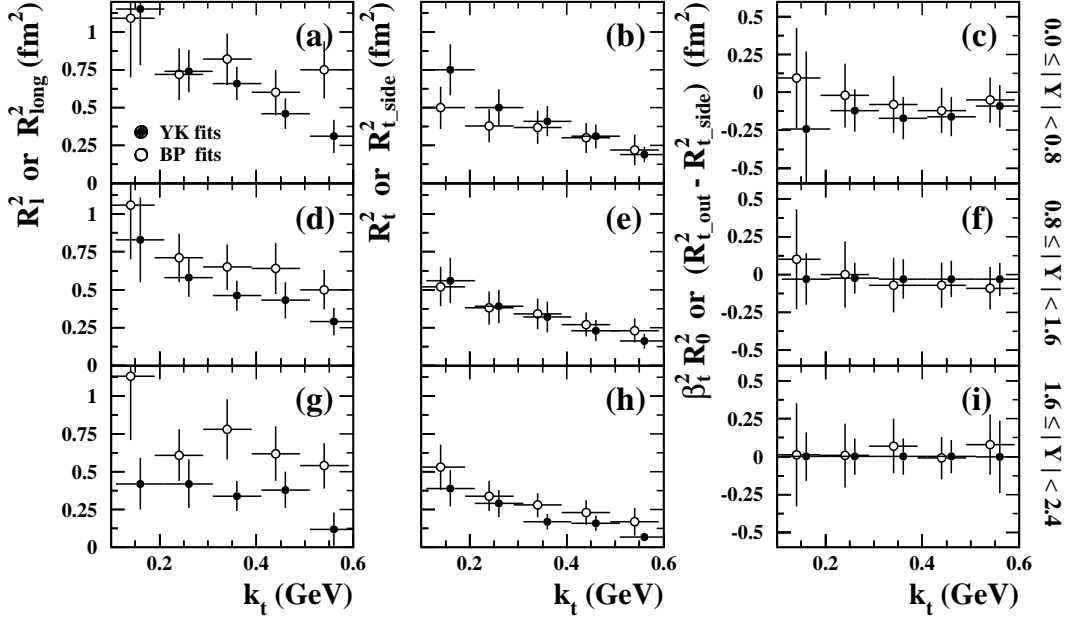


Figure 10: BP and YK fits. (a)(d)(g) The best-fit longitudinal radius R_{long}^2 in the BP frame (open dots) compared with the YK R_{ℓ}^2 (full dots). (b)(e)(h) The BP transverse correlation length R_{side}^2 (open dots) compared with the YK R_t^2 (full dots). (c)(f)(i) The difference of the BP transverse radii ($R_{\text{t,out}}^2 - R_{\text{t,side}}^2$) (open dots) compared with the YK time parameter R_0^2 times β_t^2 (full dots).

- [3] M. Cuffiani and G. Giacomelli, Il Nuovo Saggiatore 18 N1-2 (2002) 46.
- [4] P. D. Acton et al., Phys. Lett. B267 (1991) 143.
- [5] G. Abbiendi et al., Phys. Lett. B559 (2003) 131. M. Boutemour et al., hep-ex/0510027.
- [6] P. D. Acton et al., Phys. Lett. 298 (1993) 456. G. Abbiendi et al., Eur. Phys. J. C21 (2001) 23. R. Akers et al., Z. Phys. C67 (1995) 389. G. Abbiendi et al., Eur. Phys. J. C8 (1999) 559.
- [7] G. Alexander et al., Phys. Lett. B452 (1999) 159.
- [8] G. Alexander et al., Z. Phys. C72 (1996) 389. G. Giacomelli, Nucl. Phys. Proc. Suppl. 25B (1991) 30. A. Breakstone et al., Phys. Lett. B162 (1985) 400.
- [9] K. Ackerstaff et al., Eur. Phys. J. C5 (1998) 239. G. Abbiendi et al., Phys. Lett. B523 (2001) 35.
- [10] G. Abbiendi et al., Eur. Phys. J. C16 (2000) 423. M. Acciarri et al., Phys. Lett. B458 (1999) 517. P. Abreu et al., Phys. Lett. B471 (2000) 460. D. Abbaneo et al. Eur. Phys. J. C36 (2004) 147.
- [11] G. Abbiendi et al., Eur. Phys. J. C8 (1999) 59; Eur. Phys. J. C36 (2004) 297.
- [12] D. Allasia et al., Z. Phys. C37 (1988) 527.
- [13] G. Abbiendi et al., arXiv:0708.1122 [hep-ex], Eur. Phys. J. C52 (2007) 787.
- [14] K. Ahmet et al., Nucl. Instrum. Meth. A305 (1991) 275.
- [15] M. M. Aggraval et al. [WA98 Coll] Phys. Rev. Lett. 93 (2004) 022301. S. Kniese et al. [NA49 Coll] J. Phys. G30 (2004) S 1073.
- [16] J. Adams et al. [Star Coll] arXiv: nucl-ex/0411036. P. Chung et al. [Phenix Coll] Nucl. Phys. A749 (2005) 275.
- [17] K. Geiger et al., Phys. Rev. D61 (2000) 054002.
- [18] T. Csörgö, J. of Phys. Conf. Series 50 (2006) 259.